Atmospheric
Chemistry
and Physics
Discussions

Open Access

Gas and aerosol carbon in California: comparison of measurements and model predictions in Pasadena and Bakersfield

K. R. Baker[1], A. G. Carlton[2], T. E. Kleindienst[3], J. H. Offenberg[3], M. R. Beaver[3], D. R. Gentner[4], A. H. Goldstein[5], P. L. Hayes[6], J. L. Jimenez[7], J. B. Gilman[8], J. A. de Gouw[8], M. C. Woody[3], H. O. T. Pye[3], J. T. Kelly[1], M. Lewandowski[3], M. Jaoui[9], P. S. Stevens[10], W. H. Brune[11], Y.-H. Lin[12], C. L. Rubitschun[12], and J. D. Surratt[12]

[1]Office of Air Quality Planning and Standards, US Environmental Protection Agency, Research Triangle Park, NC, USA
[2]Dept. of Environmental Sciences, Rutgers University, New Brunswick, NJ, USA
[3]Office of Research and Development, US Environmental Protection Agency, Research Triangle Park, NC, USA
[4]Department of Chemical and Environmental Engineering, Yale University, New Haven, CT, USA
[5]Department of Civil and Environmental Engineering, University of California, Berkeley, CA, USA
[6]Département de Chimie, Université de Montréal, Montréal, Québec, Canada

ACPD

15, 157–198, 2015

Gas and aerosol carbon in California

K. R. Baker et al.

Title Page

Abstract	Introduction
Conclusions	References
Tables	Figures

|◀ | ▶|
◀ | ▶

Back | Close

Full Screen / Esc

Printer-friendly Version

Interactive Discussion

[7]Department of Chemistry & Biochemistry, and CIRES, University of Colorado, Boulder, CO, USA

[8]Chemical Sciences Division, Earth System Research Laboratory, National Oceanic and Atmospheric Administration, Boulder, CO, USA

[9]Alion Science and Technology, Inc., Research Triangle Park, NC, USA

[10]Center for Research in Environmental Science, School of Public and Environmental Affairs and Department of Chemistry, Indiana University, Bloomington, IN, USA

[11]Department of Meteorology, Pennsylvania State University, University Park, PA, USA

[12]Department of Environmental Sciences and Engineering, Gillings School of Global Public Health, University of North Carolina at Chapel Hill, Chapel Hill, NC, USA

Correspondence to: K. R. Baker (baker.kirk@epa.gov)

Gas and aerosol carbon in California

K. R. Baker et al.

Title Page

Abstract	Introduction
Conclusions	References
Tables	Figures

|◄ | ►|

◄ | ►

Back | Close

Full Screen / Esc

Printer-friendly Version

Interactive Discussion

Abstract

Co-located measurements of fine particulate matter ($PM_{2.5}$) organic carbon, elemental carbon, radiocarbon (^{14}C), speciated volatile organic compounds (VOCs), and OH radical during the CalNex field campaign provide a unique opportunity to evaluate the Community Multiscale Air Quality (CMAQ) model's representation of organic species from VOCs to particles. Episode averaged daily 23 h average ^{14}C analysis indicate $PM_{2.5}$ carbon at Pasadena and Bakersfield during the CalNex field campaign was evenly split between contemporary and fossil origin. CMAQ predicts a higher contemporary carbon fraction than indicated by the ^{14}C analysis at both locations. The model underestimates measured $PM_{2.5}$ organic carbon at both sites with very little (7 % in Pasadena) of the modeled mass represented by secondary production, which contrasts with the ambient based SOC/OC fraction of 63 % at Pasadena.

Measurements and predictions of gas-phase anthropogenic species, such as toluene and xylenes, are generally within a factor of 2, but the corresponding secondary organic carbon (SOC) tracer (2,3-dihydroxy-4-oxo-pentanioc acid) is systematically underpredicted by more than a factor of 2. Monoterpene VOCs and SOCs are underestimated at both sites. Isoprene is underestimated at Pasadena and over predicted at Bakersfield and isoprene SOC mass is underestimated at both sites. Systematic model underestimates in SOC mass coupled with reasonable skill (typically within a factor of 2) in predicting hydroxyl radical and VOC gas phase precursors suggests error(s) in the parameterization of semi-volatile gases to form SOC. Yield values (α) applied to semi-volatile partitioning species were increased by a factor of 4 in CMAQ for a sensitivity simulation, taking in account recent findings of underestimated yields in chamber experiments due to gas wall losses. This sensitivity resulted in improved model performance for $PM_{2.5}$ organic carbon at both field study locations and at routine monitoring network sites in California. Modeled percent secondary contribution (22 % at Pasadena) becomes closer to ambient based estimates but is still too primary compared with ambient estimates at the CalNex sites.

1 Introduction

Secondary organic aerosol (SOA) forms in the atmosphere during the gas-phase photooxidation of volatile organic compounds (VOCs) that produce semi-volatile and water-soluble gases that condense to form new particles or partition to pre-existing aerosol mass (Ervens et al., 2011). SOA contributes to the atmospheric fine particulate matter ($PM_{2.5}$) burden, with subsequent effects on air quality, visibility, and climate (Hallquist et al., 2009). Despite its importance and abundance, ambient SOA mass is not well characterized by atmospheric models. For example, the Community Multiscale Air Quality (CMAQ) model consistently underpredicts surface SOA mass concentrations for a variety of seasons and locations when compared to ambient observational estimates (Carlton and Baker, 2011; Carlton et al., 2010; Hayes et al., 2014; Zhang et al., 2014a).

SOA formation and the preceding gas-phase photooxidation chemistry are complex and often involve multiple oxidation steps in the gas, aqueous, and particle phase as well as accretion reactions in the particle phase that yield high molecular weight (MW) products. However, three-dimensional photochemical models must represent the gas-phase chemistry and SOA formation in a simplified fashion for computational efficiency (Barsanti et al., 2013). Gas-phase chemical mechanisms employ "lumped" VOC species, categorized primarily according to reactivity (e.g., reaction rate constants with $^{\bullet}OH$) (Carter, 2000; Yarwood et al., 2005), not product volatility or solubility. Condensable SOA-forming oxidation products are typically represented with 2 products in the standard versions of publically available and routinely applied photochemical modeling systems such as GEOS-CHEM (Chung and Seinfeld, 2002; Henze and Seinfeld, 2006) and WRF-CHEM (Grell et al., 2005) and those employed in regulatory applications for rulemaking such as CMAQ (Carlton et al., 2010) and the Comprehensive Air Quality Model with extensions (CAMx) (ENVIRON, 2014). Given the direct relationship between precursor VOC and OH radical abundance and SOA formation, it is important to simultaneously evaluate the model representation of all three, in particular, within the

context of how organic species evolve in the atmosphere to diagnose persistent SOA model bias.

Recent studies have shown that warm season SOA mass concentrations are usually greater than primary organic aerosol (POA) mass in the Los Angeles (Docherty et al., 2008; Hersey et al., 2011; Hayes et al., 2013) and Bakersfield (Liu et al., 2012) areas. Gas-to-particle condensation of VOC oxidation products dominate formation of summer SOA in Bakersfield (Liu et al., 2012; Zhao et al., 2013) and up to a third of nighttime organic aerosols (OA) in Bakersfield are organic nitrates (Rollins et al., 2012). Sources of warm season OA in Bakersfield include fossil fuel combustion, vegetative detritus, petroleum operations, biogenic emissions, and cooking (Liu et al., 2012; Zhao et al., 2013). Despite numerous studies based on observations and models, less consensus exists regarding the largest sources of warm season SOA at Pasadena. Bahreini et al. (2012) concluded that SOA at Pasadena is largely derived from gasoline engines with minimal biogenic and diesel fuel contribution (Bahreini et al., 2012). Others concluded large contributions from gasoline fuel combustion to SOA but also found notable contributions from diesel fuel combustion, cooking, and other sources (Gentner et al., 2012; Hayes et al., 2013). Zotter et al. (2014) conclude that 70 % of the SOA in the urban plume in Pasadena is due to fossil sources, and that at least 25 % of the non-fossil carbon is due to cooking sources.

Chemical measurements of $PM_{2.5}$ carbon, fossil and contemporary aerosol carbon fraction, OC and its components, SOC tracers and speciated VOCs taken as part of the 2010 California Research at the Nexus of Air Quality and Climate Change (CalNex) field study in central and southern California (Ryerson et al., 2013) provide a unique opportunity to quantitatively evaluate modeled organic predictions. These special study data combined with routine $PM_{2.5}$ OC measurements in California are compared with model estimates to gauge how well the modeling system captures the gas and aerosol carbon burden using the standard CMAQ aerosol approach. The SOC mechanism in the base version of CMAQ lends itself well to comparison with chemical tracers because it retains chemical identity traceable to the precursor VOC (Carlton et al., 2010).

Finally, a CMAQ sensitivity simulation was performed where the yields of semi-volatile gases from VOC oxidation were increased by a factor of 4 (Zhang et al., 2014b) to determine whether this may ameliorate the model underprediction of secondary organic carbon (SOC) seen here and in other studies (Ensberg et al., 2014).

2 Methods

Predictions of speciated VOC, speciated SOC, and aerosol-phase carbon are simultaneously compared to co-located ambient measurements at two surface locations, one in Los Angeles County (Pasadena) and one in the San Joaquin Valley (Bakersfield) air basin. The CMAQ photochemical model is applied with a fine grid resolution (4 km sized grid cells) using emissions from the 2011 National Emissions Inventory and 2010 specific point source information where available.

2.1 Model application

The model domain covers the State of California and part of northwest Mexico using 4 km square sized grid cells (Fig. S1 in the Supplement). The vertical domain extends to 50 mb using 34 layers (layer 1 top ∼ 35 m) with most resolution in the boundary layer. Initial and boundary conditions are from a coarser CMAQ simulation that used 3 hourly varying input from a global GEOS-Chem (v8-03-02) global model (http://acmg.seas.harvard.edu/geos/) simulation for the same period (Henderson et al., 2014). Gridded meteorological variables are generated using the Weather Research and Forecasting model (WRF), Advanced Research WRF core (ARW) version 3.1 (Skamarock et al., 2008). Surface meteorology including temperature, wind speed, and wind direction and daytime mixing layer height was well characterized by WRF in central and southern California during this period (Baker et al., 2013).

Hourly solar radiation and temperature estimated by the WRF model are used as input to the Biogenic Emission Inventory System (BEIS) v3.14 to generate hourly

emissions estimates of biogenic speciated VOC and NO (Carlton and Baker, 2011). Electric generating point source emissions that report continuous emissions monitor (CEM) data are used in the modeling to reflect 2010 emissions information. Day specific fires are represented but minimally impacted air quality during this period (Hayes et al., 2013). Mobile source emissions were interpolated between totals provided by the California Air Resources Board for 2007 and 2011. Other anthropogenic emissions are based on the 2011 National Emissions Inventory (NEI) version 1 (United States Environmental Protection Agency, 2014). Primary mass associated with carbon (non-carbon organic mass, NCOM) is estimated based on sector specific organic matter-to-organic carbon (OM : OC) ratios (Simon and Bhave, 2012). Emissions are processed to hourly gridded input for CMAQ with the Sparse Matrix Operator Kernel Emissions (SMOKE) modeling system (http://www.cmascenter.org/smoke/).

Emissions of primarily emitted $PM_{2.5}$ OC and the sum of anthropogenic SOA precursors benzene, toluene, and xylenes (BTX) are shown in Table 1 by source sector and area. Here, the southern San Joaquin valley includes emissions from Kern, Tulare, Kings, and Fresno counties and the Los Angeles area include emissions from Los Angeles and Orange counties. Green shading indicates the sector for that area is dominated by contemporary carbon emissions. BTX emissions in both areas are dominated by mobile sources (onroad and offroad) and area sources such as solvent utilization and waste disposal (Table S1). Primary OC emissions are largely commercial cooking (non-point area) in both locations with notable contribution from various types of stationary point and mobile sources. BTX emissions are almost completely fossil in origin and primarily emitted OC is split fairly evenly between contemporary and fossil origin in these areas based on the 2011 version 1 NEI (Table 1).

2.2   Model background

CMAQ version 5.0.2 (www.cmaq-model.org) was applied to estimate air quality in California from 5 May to 1 July 2010, coincident with the CalNex Study. Gas-phase chemistry is simulated with the SAPRC07 mechanism (Hutzell et al., 2012) and aqueous-

Title Page

Abstract | Introduction

Conclusions | References

Tables | Figures

◄ | ►

◄ | ►

Back | Close

Full Screen / Esc

Printer-friendly Version

Interactive Discussion

phase chemistry that oxidizes sulfur, methylglyoxal, and glyoxal (Carlton et al., 2008; Sarwar et al., 2013). The AERO6 aerosol chemistry module includes ISORROPIAII (Fountoukis and Nenes, 2007) inorganic chemistry and partitioning. The modeling system generally does well capturing ambient inorganic gases and $PM_{2.5}$ species during this time period at Pasadena and Bakersfield (Kelly et al., 2014; Markovic et al., 2014).

Model predicted OC species are shown in Fig. 1 by volatility bin (log of C^*) and O : C ratio (see Supplement for related details). Aqueous-phase species are shown with blue circles, species largely fossil in origin are colored brown and those non-fossil in origin are green. A general trend of increasing O : C ratio as volatility decreases is consistent with laboratory and field measurements (Jimenez et al., 2009). The placement of the MGLY gem-diol vertically above gas-phase MGLY in Fig. 1 represents hydration processes. Aqueous-phase organic chemistry represents both functionalization and oligomerization because some photooxidation products are small carboxylic acids and others are high MW species (Tan et al., 2010; Carlton et al., 2007).

VOC precursors for SOA include isoprene, monoterpenes, sesquiterpenes, xylenes, toluene, benzene, alkanes, glyoxal, and methylglyoxal (Fig. 1 right panel). Benzene, toluene, and xylene form SOA precursors with high-NO_X ($RO_2 + NO$) and low-NO_X ($RO_2 + HO_2$) specific yields (Carlton et al., 2010). CMAQ converts these precursors into multiple semi-volatile products (Fig. 1 middle panel) after a single oxidation step. These multiple products vary in terms of assigned volatility and oxygen-to-carbon (O : C) ratio. All semi-volatile SOA mass oligomerizes in CMAQ. After this process SOA identity is classified only as anthropogenic or biogenic, dependent on the VOC precursor (see Fig. S2). After oligomerization, the saturation vapor pressure (C^*) and OM : OC ratio associated with all of the 2-product semi-volatile SOA species change from the individual values to the values assigned for non-volatile, non-partitioning oligomerized SOA mass ($C^* \approx 0$; OM : OC = 2.1) (Carlton et al., 2010).

CMAQ VOCs and SOC species are paired in time and space with measurements (Table S2). Modeled predictions are averaged temporally to match observations and extracted from the grid cell where the monitor is located. Modeled toluene and

xylene SOC are aggregated to match the measured SOC tracer (2,3-dihydroxy-4-oxopentanoic acid) which is known to represent products from both compounds and potentially other methylated aromatics (Kleindienst et al., 2004). Because the original VOCs contributing to oligomerized species are not tracked by CMAQ, biogenic oligomerized species mass is apportioned to parent VOC based on the fraction each semi-volatile SOC species contributes to the total semi-volatile (non-oligomerized) biogenic SOC at that time and location. The same technique is applied to anthropogenic SOC.

2.3 Sampling and analysis methods

CalNex ground-based measurements took place in Pasadena, CA, from 15 May–15 June 2010 and in Bakersfield, CA, from 15 May–30 June 2010. The Bakersfield sampling site was located in a transition area of southeast Bakersfield between the city center and areas of agricultural activity. The Pasadena sampling site was located on the California Institute of Technology campus with the Los Angeles metropolitan area to the southwest and San Gabriel Mountains directly north (see Fig. S3).

An ambient-based approach is used here to estimate secondary OC from individual or groups of similar hydrocarbons (Kleindienst et al., 2010). Concentrations of specific, tracer, compounds are determined and used to estimate SOC contributions from the particular source groups based on measured laboratory tracer-to-SOC mass fractions (Kleindienst et al., 2007). To conduct tracer-based organic aerosol characterization, filter-based particulate matter sampling was conducted at each site for 23 h periods starting at midnight (PDT) of the designated sampling day. In total, there were 32 filter samples from Pasadena and 36 from the Bakersfield site (Lewandowski et al., 2013). The filter sampling protocols have been described in detail elsewhere (Kleindienst et al., 2010). For the analysis of the SOC tracer compounds, filters and field blanks were treated using the derivatization method described by Kleindienst et al. (2007). The mass spectral analysis for the organic compounds used as secondary molecular trac-

ers has been described (Edney et al., 2003). The method detection limit (MDL) for the SOC tracer species is 0.1 ng m^{-3}.

OC and elemental carbon (EC) concentrations were determined using the thermal-optical transmittance (TOT) method (Birch and Cary, 1996) from 1.54 cm^2 punches of quartz filters collected concurrent with the filters used for tracer analyses (hereafter referred to as UNC/EPA OC). The outer non-loaded rings were removed from filter samples then sent to Woods Hole Oceanographic Institute Accelerator Mass Spectrometry for ^{14}C analysis. The fraction of contemporary carbon is provided for each daily total PM$_{2.5}$ carbon sample (Geron, 2009). The contemporary carbon fraction is expressed as a percentage of an oxalic acid standard material that represents the carbon isotopic ratio for wood growth during 1890 (Stuiver, 1983). To account for the atmospheric ^{14}C enhancement due to nuclear bomb testing in the 1950s and 1960s, a factor of 1.044 was used to calculate the contemporary carbon fraction from the measured modern carbon result (Lewis et al., 2004; Zotter et al., 2014). The fraction of contemporary PM$_{2.5}$ organic carbon is estimated based on Zotter et al. (2014).

Two VOC datasets (one canister based, and one in situ) from each site were used in this analysis. Three hour integrated (06:00–09:00 PDT) canister samples for VOC analysis were collected at both sites. A total of 41 samples were collected at the Bakersfield site and 31 at Pasadena. The offline VOC analysis details are given in the Supplement. In Bakersfield, online VOC mixing ratios were collected for 30 min on the hour, and analyzed via gas chromatography-flame ionization detector (GC-FID) and gas chromatography-mass spectrometry (GC-MS) (Gentner et al., 2012). In Pasadena, online VOC measurements were collected for 5 min every 30 min and analyzed via GC-MS (Borbon et al., 2013; Gilman et al., 2010). Carbon monoxide measurements at Pasadena were determined using UV fluorescence (Gerbig et al., 1999).

Hydroxyl (OH) and hydroperoxyl (HO$_2$) radical measurements were made at both locations using Fluorescence Assay with Gas Expansion (FAGE). The Bakersfield OH measurements used in this analysis were collected using the OH$_{chem}$ method from the Penn State ground-based FAGE instrument (Mao et al., 2012). The Pasadena HO$_x$

observations were made using the Indiana University FAGE instrument (Dusanter et al., 2009). HO_2 measurements from both instruments could contain an interference from various RO_2, therefore when comparing the model output with the observations, the sum of modeled HO_2 and RO_2 has been used (Griffith et al., 2013).

⁵   OC measurements from nearby Chemical Speciation Network (CSN) sites in Pasadena and Bakersfield were also used for comparison purposes. The Los Angeles CSN site (60371103) was approximately 9 miles from the CalNex site, and the Bakersfield CSN site (60290014) was approximately 3 miles from the CalNex site (see Fig. S3a and b in the Supplement). The CSN network uses quartz-fiber filters and

¹⁰ analyzes the carbon off-line using the thermal-optical reflectance method. Aerodyne High-Resolution Time-of-Flight Aerosol Mass Spectrometer (AMS) measurements of PM_1 OC made at Pasadena are described in Hayes et al. (2013) and online Sunset $PM_{2.5}$ OC measurements made at Bakersfield are described in Liu et al. (2012).

3   Results and discussion

¹⁵ The results and discussion are organized such that the contemporary and fossil components of $PM_{2.5}$ carbon at the Pasadena and Bakersfield sites are discussed, followed by model performance for $PM_{2.5}$ carbon, speciated VOC, and SOC tracer groups. Table 2 shows episode aggregated model performance metrics for $PM_{2.5}$ organic and elemental carbon, SOC tracers, total VOC, and select VOC species. The results of

²⁰ a sensitivity increasing semi-volatile yields are presented throughout and discussed in detail before finally providing an evaluation of $PM_{2.5}$ carbon at all routine monitor sites in California.

3.1   Contemporary and fossil origins of $PM_{2.5}$ carbon

Field campaign average total $PM_{2.5}$ carbon measurements indicate nearly equal

²⁵ amounts of contemporary and fossil contribution at Pasadena and Bakersfield. The

field study average contemporary fraction of 23 h average $PM_{2.5}$ total carbon samples is 0.51 at Bakersfield ($N = 35$) and 0.48 at Pasadena ($N = 25$). The estimate for contemporary carbon fraction at Pasadena is consistent with other ^{14}C measurements at this location for this period (Zotter et al., 2014) and similar to measurements made at urban areas in the Southeast United States: Birmingham 52 % and Atlanta 63 % contemporary carbon (Kleindienst et al., 2010).

Figure 2 shows observed daily 23 h average elemental carbon and OC shaded by contemporary and fossil component. The fractional contribution of contemporary carbon to total $PM_{2.5}$ carbon is variable from day-to-day at the Pasadena site and steadily increases through the study period at the Bakersfield location (first week average of 0.44 and final week average of 0.58). Some of the contemporary carbon fraction measurements from Pasadena were above 1.0. These samples were considered erroneous and not included in the analysis and suggest the possibility of positive biases due to nearby sources (e.g. medical incinerator) in the area. It is possible some of the stronger day-to-day variability in contemporary carbon fraction measurements at Pasadena may be related to biases due to nearby "hot" sources. Higher time resolution ^{14}C measurements at Pasadena show an increase in fossil fraction during the middle of the day related to increased emissions of fossil $PM_{2.5}$ carbon precursors and SOA formation in the Los Angeles area (Zotter et al., 2014). $PM_{2.5}$ OC of fossil origin at Pasadena shows the strongest relationship to daily average temperature (Fig. S4a) compared with contemporary carbon, total carbon, and elemental carbon. At Bakersfield the relationship between daily average temperature and fossil and contemporary carbon is similar (Fig. S4b) and not as strong as the relationship in Pasadena. Neither fossil nor contemporary carbon concentrations show discernible patterns by day of the week at either location (Fig. S5).

Episode average ambient estimates of $PM_{2.5}$ OC contemporary fraction (Bakersfield = 0.51 and Pasadena = 0.48) are similar to the estimated contemporary fraction of the urban emissions of primary $PM_{2.5}$ OC (Bakersfield = 0.53 and Pasadena = 0.51), as noted in Table 1. Modeled contemporary $PM_{2.5}$ carbon is estimated by summing pri-

marily emitted PM$_{2.5}$ multiplied by the contemporary fraction of urban area emissions (see Sect. 2.1 and Table 1) with model estimated biogenic SOC species. The average baseline modeled contemporary fraction of PM$_{2.5}$ OC in Pasadena is 0.51 and Bakersfield 0.54, both of which are similar to average observation estimates. However, the model shows little day to day variability in contemporary carbon fraction which does not match observed trends (Fig. S6).

3.2 PM$_{2.5}$ carbon

Figure 3 shows measured (UNC/EPA data) and modeled PM$_{2.5}$ OC at Bakersfield and Pasadena. Organic carbon measurements from co-located instruments (AMS at Pasadena measured PM$_1$ and Sunset at Bakersfield measured PM$_{2.5}$) and a nearby CSN monitor are also shown in Fig. 3. The co-located AMS measurements compare well with the UNC/EPA PM$_{2.5}$ organic carbon measurements at Pasadena, while the concentrations measured at the nearby CSN site are substantially lower. At Bakersfield UNC/EPA measurements compared with the nearby CSN (episode average ∼ 3 times lower) and co-located daily average Sunset (episode average 20 % lower) measured PM$_{2.5}$ OC illustrate possible measurement artifacts in the CalNex measurements at this location. These differences in measured concentration at Bakersfield may be related to filter handling, variability in collected blanks, true differences in the OC concentrations since the CSN site is spatially distinct, differences in the height of measurement (these CSN monitors are situated on top of buildings), and differences in analytical methods since CSN sites use the thermal optical reflectance (TOR) to operationally define OC and EC.

PM$_{2.5}$ OC is underestimated at both CalNex locations (Fig. 3), most notably at Bakersfield. However, given the large differences in PM$_{2.5}$ OC mass compared to co-located and nearby routine measurements, it is not clear which measurement best represents ambient PM$_{2.5}$ OC concentrations and would be most appropriate for comparison with the model. The model generally compares well to the CSN site nearest Pasadena and Bakersfield. PM$_{2.5}$ elemental carbon is well characterized by the model

at Bakersfield (fractional bias = −13 % and fractional error = 35 %) and over-estimated at Pasadena (fractional bias and error = 125 %) (Fig. S7). Since the emissions are based on TOR and UNC/EPA measurements use the TOT operational definition of total carbon some of the model overestimation may be related to the TOR method estimating higher elemental carbon fraction of total carbon (Chow et al., 2001).

PM$_{2.5}$ OC is mostly primary (Pasadena 93 % and Bakersfield 88 %) in the baseline model simulation. AMS measurements at Pasadena suggest OC is mostly secondary in nature with an average of 63 % for the SVOOA and OOA components for this field study (Hayes et al., 2013). Model estimated PM$_{2.5}$ OC is largely from primarily emitted sources and contemporary in nature based on the contemporary/fossil split of primary PM$_{2.5}$ emissions near both sites (Fig. S6). Primarily emitted PM$_{2.5}$ OC emissions sources near Pasadena and Bakersfield include mobile sources, cooking, and dust based on emissions inventory information (Table 1). Some of these sources of primarily emitted PM$_{2.5}$ OC may be semi-volatile in nature. Model treatment of POA as semi-volatile may improve the primary–secondary comparison with observations but would likely exacerbate underpredictions of PM$_{2.5}$ OC, unless oxidation and re-partitioning of the products is considered (Robinson et al., 2007). The underestimation of SOC may result from underestimated precursor VOC, poorly characterized oxidants, underestimated semi-volatile yields, other issues, or some combination of each.

3.3 Gas-phase carbon

Model estimates are paired with hourly VOC (Fig. S8) and mid-morning 3 h average VOC (Fig. S9) at both locations. Compounds considered largely fossil in origin including xylene, toluene, and benzene are generally well predicted at both sites although these species tend to be slightly overestimated at Pasadena and slightly underestimated at Bakersfield. Since emissions of these compounds near these sites are mostly from mobile sources (Table 1), this suggests emissions from this sector are fairly well characterized in this application.

Contemporary (biogenic) origin monoterpenes are underestimated at both sites while isoprene is underestimated at Pasadena and has little bias at Bakersfield based on hourly measurements (Fig. S8; Table 2). Isoprene and monoterpene performance may be related to deficiencies in emissions factors, vegetation characterization, or poorly characterized meteorology that may not capture transport from nearby large emitting vegetation to these monitor locations. Speciated monoterpene measurements made at Bakersfield during this field campaign suggest emissions of certain species were elevated at the start of this time period due to flowering (Gentner et al., 2014b), which is a process not included in current biogenic emissions models thus it may contribute to modeled monoterpene underestimates.

Other VOC species that are systematically underestimated include ethane, methanol, ethanol, and acetaldehyde. Underprediction of methanol and ethanol in Bakersfield may be largely related to missing VOC emissions for confined animal operations in the emission inventory (Gentner et al., 2014a). Underestimates of oxygenated VOC compounds may indirectly impact SOC formation through muted photochemistry (Steiner et al., 2008). Carbon monoxide tends to be underestimated at both locations (Fig. S8), possibly due to boundary inflow concentrations from the global model simulation being too low.

3.4 PM$_{2.5}$ SOC tracers

Figure 4 shows modeled and measured total PM$_{2.5}$ OC mass. Measured mass explained by fossil and contemporary SOC tracers are shown in the top row. Modeled mass is similarly colored to show the amount explained by modeled SOC. The observed unexplained fraction origins are a mixture of primary, secondary, fossil and contemporary origin. The modeled unexplained fraction represents primarily emitted PM$_{2.5}$ OC. Estimates of SOC mass from a specific or lumped VOC group (e.g. isoprene, monoterpenes, toluene) as estimated by specific tracer species, hereafter called SOC tracer mass, comprise little of the measured or modeled PM$_{2.5}$ OC at either of these locations during this field study (Fig. 4). Total SOC tracer estimates explain only 9 %

of the total measured UNC/EPA $PM_{2.5}$ OC at Pasadena and 5 % at Bakersfield. The percentage of mass explained by known secondary tracers is smaller than urban areas in the southeast United States: Atlanta 27 % and Birmingham 31 % (Kleindienst et al., 2010). The portion of measured and modeled $PM_{2.5}$ carbon not identified with tracers may be from underestimated adjustment factors related to previously uncharacterized SVOC wall loss in chamber studies (Zhang et al., 2014b), unidentified SOC pathways, known pathways without an ambient tracer, and tracer degradation between formation and measurement. Based on ^{14}C measurements, this unidentified portion of the measurements is likely comprised of both contemporary and fossil carbon in generally similar amounts. Total modeled SOC explain only 12 % of the $PM_{2.5}$ carbon at Bakersfield and 7 % at Pasadena. As noted previously, AMS based observations suggest most OC is SOC (63 %) at Pasadena (Hayes et al., 2013) meaning both the SOC tracer measurements and model estimates explain little of the SOC at this location.

Despite the relatively small component of total $PM_{2.5}$ carbon explained by SOC tracers, a comparison of measured and modeled SOC and precursor VOC provides additional opportunity to better understand sources of $PM_{2.5}$ carbon in these areas and begin to establish relationships between precursors and resulting SOC formation. Ambient and model estimated SOC tracers and daily average VOC precursors are shown in Fig. 5 for Pasadena and Fig. 6 for Bakersfield. The model underestimates toluene and xylene SOC at both locations even though the VOC gas precursors show an over-prediction tendency at Pasadena and slight underestimation at Bakersfield. Isoprene SOC is generally under predicted at both sites, in particular at Bakersfield. This is in contrast to the slight overprediction of daily 24 h average isoprene at Bakersfield. One explanation may be that isoprene SOC is formed elsewhere in the region (e.g. the nearby foothills of the Sierra Nevada where emissions are highest in the region), which would support the lack of relationship between isoprene SOC and isoprene concentrations at Bakersfield (Shilling et al., 2013). The lack of relationship could also be related to the reactive uptake kinetics of isoprene-derived epoxydiols (IEPOX) (Gaston et al., 2014) and methacrylic acid epoxide (MAE). Since the model does not include

Gas and aerosol carbon in California

K. R. Baker et al.

the reactive uptake of IEPOX and MAE and subsequent acid-catalyzed aqueous phase chemistry it is likely isoprene SOC would be underestimated to some degree at both sites (Karambelas et al., 2013; Pye et al., 2013). Of these channels the IEPOX channel is thought to have the largest SOA production potential, but the chemistry in the LA

5   basin proceeds almost completely through the high-NO channel (Hayes et al., 2014), and thus IEPOX is not formed from isoprene emitted within the LA basin. Consistent with that observation, the AMS tracer of IEPOX SOA is only detected at background level in the LA basin.

Monoterpene VOC and monoterpene SOC are underestimated systematically at
10 both locations suggesting underpredictions of the VOC precursor translates to underestimates in SOC. As noted previously, monoterpene measurements suggest an emissions enhancement related to flowering or other emission events (e.g. harvest or pruning) (Gentner et al., 2014b) that is not included in current biogenic emissions model formulations. The monoterpene measured tracer SOC group is based on α-

15 pinene products. Measured SOC at these sites could be from monoterpene species other than α-pinene. A coincident study near Bakersfield indicates α- and β-pinene emissions represent a fairly small fraction of total monoterpene emissions during this time period (Gentner et al., 2014b). SOA yields in CMAQ for monoterpenes are heavily weighted toward α- and β- pinene, which may be appropriate in most places, but

20 not here where measurements show large contributions from limonene, myrcene, and para-cymene.

Sesquiterpene VOC and SOC tracer (β-caryophyllenic acid) mass measurements were never above the MDL at either site during CalNex, but the modeling system often predicts SOC from this VOC group (Table 2, Fig. S10b). The SOC tracer measurement

25 methodology is more uncertain for sesquiterpene products (Offenberg et al., 2009) and gas-phase sesquiterpenes would have oxidized before reaching the measurement sites since sesquiterpene emitting vegetation exists in the San Joaquin Valley (Ormeño et al., 2010). It is also possible that SOC is forming from sesquiterpenes other than β-caryophyllene.

One potential explanation for an underestimation of SOC despite well characterized precursors (e.g. toluene and xylenes) could be lack of available oxidants. As shown in Fig. 7, the model tends to overestimate the hydroxyl radical compared with measurement estimates at Pasadena. Hydroperoxyl + peroxy radical measurements are underestimated at Pasadena by a factor of 2 on average. The model overestimates preliminary measurements of both hydroxyl (by nearly a factor of 2 on average) and hydroperoxyl + peroxy radicals at Bakersfield. Model representation of hydroxyl radical at these locations during this time period does not seem to be limiting VOC oxidation to semi-volatile products. Hydroperoxyl underestimates at Pasadena could lead to muted SOA formation through low-NO_X pathways dependent on hydroperoxyl concentrations and contribute to model under-estimates of SOC.

3.5 Sensitivity simulation

OH is not underestimated in the model and biases in precursor VOC do not clearly translate into similar biases in SOC (e.g. toluene and xylene VOC are overestimated at Pasadena but tracer SOC for this group is underestimated) for these sites during this time period. Modeled SOC may partly be underestimated due to the use of experimental SOC yields that may be biased low due to chamber studies not fully accounting for SVOC wall loss (Zhang et al., 2014b). Even though Zhang et al. (2014b) showed results for one precursor to SOA pathway, as a sensitivity study here the yield of all semivolatile gases are increased by a factor of 4. This was done by increasing in the mass-based stoichiometric coefficients for each VOC to SOA pathway in the model to provide a preliminary indication about how increased yields might impact model performance. A factor of 4 is chosen based on the upper limit related to SVOC wall loss in (Zhang et al., 2014b). Aside from wall loss characterization, there are a variety of other aspects of chamber studies that could result in underestimated yields including particle-phase accretion and aqueous phase chemistry and differences in chamber and ambient humidity.

Model estimates of PM$_{2.5}$ OC increase in urban areas and regionally when semivolatile yields are increased. The sensitivity simulation results in episode average anthropogenic SOC increases by a factor of 3 (benzene SOC at Pasadena) to 4.8 (toluene and xylene SOC at Pasadena) and biogenic SOC increases between a factor of 5.1 (isoprene SOC at Pasadena) to 8.9 (monoterpene SOC at Bakersfield). Model performance improves at the CalNex locations (Figs. 3 and 4) and at routine monitors throughout California (Fig. 8). Average fractional bias improves from −63 to −25 % at routine monitor locations and fractional error is reduced from 75 to 51 %.

The sensitivity simulation with increased semivolatile yields results in increased model estimated secondary contribution as a percent of total PM$_{2.5}$ carbon, but still does not conform to observation based estimates that indicate PM$_{2.5}$ carbon is largely secondary in nature at these sites (Liu et al., 2012; Hayes et al., 2013). Modeled SOC in the sensitivity simulation explains 36 % of the PM$_{2.5}$ OC at Bakersfield and 22 % at Pasadena, which is larger than the baseline simulation by more than a factor of 3. The model predicted percent contemporary fraction of PM$_{2.5}$ carbon changed very little due to this sensitivity. The model sensitivity results are not compared to SOC tracer group estimates since the conversion of tracer concentrations to SOC concentrations would require a similar adjustment and would result in similar relationships between model estimates and observations.

3.6   Aqueous and other SOC processes

Measurements in Pasadena during the summer of 2009 suggest aqueous processes can be important for SOC mass (Hersey et al., 2011). For the CalNex period at Pasadena, Washenfelder et al. (2012) showed box model estimated 8 h average SOC from aqueous-phase chemistry of glyoxal to be between 0.0 and 0.2 µg m^{-3} (Washenfelder et al., 2011) and Hayes et al. (2014) showed that the observed SOA was not different between cloudy and clear morning days. CMAQ predicted 24 h average SOC from glyoxal and methygloxal through aqueous chemistry at Pasadena ranges from 0.0

to 0.04 µg m^{-3}. CMAQ estimates of SOC from small carbonyl compounds via aqueous-phase processes are within the range inferred from measurements.

Not all CMAQ SOC formation pathways can be included in this analysis. No observational indicator exists for SOC derived from alkanes, benzene, glyoxal, and methyl-glyoxal since unique tracer species have not been determined. Conversely, naphthalene/PAH SOC tracers were measured, but not modeled in CMAQ. Measured naphthalene SOC at these sites is minor (Hayes et al., 2014) which is consistent with other areas (Dzepina et al., 2009). Previous CMAQ simulations predict that PAHs contribute less than 30 ng m^{-3} of SOA in Southern California in summer (Pye and Pouliot, 2012), and thus including those pathways is unlikely to close the model-measurement gap in total OC. 2-Methyl-3-Buten-2-ol (MBO) derived SOC concentrations (3–4 ngC m^{-3}) were low at both monitor locations throughout the campaign (Lewandowski et al., 2013). MBO does not appear to notably contribute SOC at these locations during this time period, which is consistent with low yields estimated in laboratory experiments (Chan et al., 2009). Organic carbon emitted from marine biological activity is not included in this modeling assessment and may contribute to some degree at Pasadena (Gantt et al., 2010) based on ship-based measurements (Hayes et al., 2013).

3.7 Regional PM$_{2.5}$ organic carbon

Including routine measurement data is important to characterize model performance beyond the two CalNex monitor locations and provide broader context for PM$_{2.5}$ carbon in California and understand how the model performs and responds to perturbations at diverse locations. The highest average modeled PM$_{2.5}$ OC in California during this period is in the Los Angeles area (Fig. 8). The Sacramento and San Joaquin valleys also show higher concentrations of PM$_{2.5}$ OC than more rural parts of the State (Fig. 8). Measurements made at routine monitor networks (Fig. 8) show similar elevated concentrations near Los Angeles, Sacramento valley, and San Joaquin valley. These areas of elevated OC generally coincide with areas of the State that experience

a build-up of pollutants due to terrain features blocking air flow (Baker et al., 2013). The model does not tend to capture the highest concentrations of measured $PM_{2.5}$ OC in the central San Joaquin valley, Imperial Valley, or at one CSN monitor in the northeast Sierra Nevada that is near large residential wood combustion emissions (Fig. S11). The model underestimates $PM_{2.5}$ OC on average across all CSN sites during this time period (fractional bias = −63 % and fractional error = 75 %). The modeling systems show a slight overprediction tendency (fractional bias = 27 %) across all CSN sites for $PM_{2.5}$ elemental carbon in California during this period.

4 Conclusions

Total $PM_{2.5}$ carbon at Pasadena and Bakersfield during the CalNex period in May and June of 2010 is fairly evenly split between contemporary and fossil origin. Total $PM_{2.5}$ OC is generally underestimated at both field study locations and at many routine measurement sites in California. Comparison with AMS observations at CalNex sites suggest a large underestimate of SOC. Semivolatile yields were increased by a factor of 4 based on recent research suggesting yields may be higher due to updated accounting for SVOC wall loss. This sensitivity resulted in a better comparison to routine and field study measurements. However, the model estimated OC is still largely primary in nature and inconsistent with observation based approaches at CalNex sites.

CMAQ predictions of individual VOCs are often not consistent with model performance for the corresponding subsequent SOC species mass. Gas-phase mixing ratios of toluene and xylene are well-predicted by CMAQ, typically within a factor of 2 of the observations at both sites. However, measurement-based estimates of the corresponding SOC mass are consistently greater than model-predicted mass. Mass concentrations of isoprene SOC are systematically underpredicted, most noticeably at Bakersfield, while model predictions of gas-phase isoprene are not biased in only one direction to the same degree. Gas-phase monoterpenes and the related SOC species are underpredicted at both CalNex monitoring sites. The hydroxyl radical is fairly well

Gas and aerosol carbon in California

K. R. Baker et al.

Back | Close

Full Screen / Esc

Printer-friendly Version

Interactive Discussion

Discussion Paper | Discussion Paper | Discussion Paper | Discussion Paper

characterized at Pasadena and systematically overestimated at Bakersfield suggesting oxidants are not limiting SOC production in the model.

Episode average CMAQ model estimates of $PM_{2.5}$ OC contemporary fraction at Pasadena and Bakersfield are similar to radiocarbon measurements but lack day to day variability. CMAQ $PM_{2.5}$ OC is predominantly primary in origin which is contrary to findings from other studies that $PM_{2.5}$ OC in these areas are largely secondary in nature during this time period (Bahreini et al., 2012; Hayes et al., 2013; Liu et al., 2012). Treatment of primarily emitted $PM_{2.5}$ OC as semi-volatile would likely result in total $PM_{2.5}$ OC estimates that would be mostly secondary rather than primary. Some model performance features including underestimated SOC may be related to less volatile hydrocarbons emitted from some source categories missing from the emission inventory (Chan et al., 2013; Gentner et al., 2012; Jathar et al., 2014) or mischaracterized when lumped into SAPRC VOC species (Jathar et al., 2014). A future intent is to simulate this same period using a volatility basis set approach to treat primary OC emissions with some degree of volatility and potential for SOC production and better account for sector specific intermediate volatility emissions.

The Supplement related to this article is available online at doi:10.5194/acpd-15-157-2015-supplement.

Disclaimer. Although this work was reviewed by EPA and approved for publication, it may not necessarily reflect official Agency policy.

References

Bahreini, R., Middlebrook, A. M., de Gouw, J. A., Warneke, C., Trainer, M., Brock, C. A., Stark, H., Brown, S. S., Dube, W. P., Gilman, J. B., Hall, K., Holloway, J. S., Kuster, W. C., Perring, A. E., Prevot, A. S. H., Schwarz, J. P., Spackman, J. R., Szidat, S., Wagner, N. L., Weber, R. J., Zotter, P., and Parrish, D. D.: Gasoline emissions dominate over diesel in formation of secondary organic aerosol mass, Geophys. Res. Lett., 39, L06805, doi:10.1029/2011gl050718, 2012.

Baker, K. R., Misenis, C., Obland, M. D., Ferrare, R. A., Scarino, A. J., and Kelly, J. T.: Evaluation of surface and upper air fine scale WRF meteorological modeling of the May and June 2010 CalNex period in California, Atmos. Environ., 80, 299–309, 2013.

Barsanti, K. C., Carlton, A. G., and Chung, S. H.: Analyzing experimental data and model parameters: implications for predictions of SOA using chemical transport models, Atmos. Chem. Phys., 13, 12073–12088, doi:10.5194/acp-13-12073-2013, 2013.

Birch, M. and Cary, R.: Elemental carbon-based method for monitoring occupational exposures to particulate diesel exhaust, Aerosol Sci. Tech., 25, 221–241, 1996.

Borbon, A., Gilman, J., Kuster, W., Grand, N., Chevaillier, S., Colomb, A., Dolgorouky, C., Gros, V., Lopez, M., and Sarda-Esteve, R.: Emission ratios of anthropogenic volatile organic compounds in northern mid-latitude megacities: observations vs. emission inventories in Los Angeles and Paris, J. Geophys. Res.-Atmos., 118, 2041–2057, 2013.

Carlton, A. G. and Baker, K. R.: Photochemical modeling of the Ozark Isoprene Volcano: MEGAN, BEIS, and their impacts on air quality predictions, Environ. Sci. Technol., 45, 4438–4445, doi:10.1021/es200050x, 2011.

Carlton, A. G., Turpin, B. J., Altieri, K. E., Reff, A., Seitzinger, S., Lim, H. J., and Ervens, B.: Atmospheric oxalic acid and SOA production from glyoxal: results of aqueous photooxidation experiments, Atmos. Environ., 41, 7588–7602, 2007.

Carlton, A. G., Turpin, B. J., Altieri, K. E., Seitzinger, S. P., Mathur, R., Roselle, S. J., and Weber, R. J.: CMAQ model performance enhanced when in-cloud SOA is included: comparisons of OC predictions with measurements, Environ. Sci. Technol., 42, 8798–8802, 2008.

Carlton, A. G., Bhave, P. V., Napelenok, S. L., Edney, E. O., Sarwar, G., Pinder, R. W., Pouliot, G. A., and Houyoux, M.: Treatment of secondary organic aerosol in CMAQv4.7, Environ. Sci. Technol., 44, 8553–8560, 2010.

Gas and aerosol carbon in California

K. R. Baker et al.

Title Page

Abstract	Introduction
Conclusions	References
Tables	Figures

|◄ | ►|
◄ | ►

Back | Close

Full Screen / Esc

Printer-friendly Version

Interactive Discussion

Carter, W. P. L.: Implementation of the SAPRC-99 Chemical Mechanism Into the Models-3 Framework, US Environmental Protection Agency, University of California, Riverside, CA, USA, 2000.

Chan, A. W. H., Galloway, M. M., Kwan, A. J., Chhabra, P. S., Keutsch, F. N., Wennberg, P. O., Flagan, R. C., and Seinfeld, J. H.: Photooxidation of 2-methyl-3-buten-2-ol (MBO) as a potential source of secondary organic aerosol, Environ. Sci. Technol., 43, 4647–4652, doi:10.1021/es802560w, 2009.

Chan, A. W., Isaacman, G., Wilson, K. R., Worton, D. R., Ruehl, C. R., Nah, T., Gentner, D. R., Dallmann, T. R., Kirchstetter, T. W., and Harley, R. A.: Detailed chemical characterization of unresolved complex mixtures in atmospheric organics: insights into emission sources, atmospheric processing, and secondary organic aerosol formation, J. Geophys. Res.-Atmos., 118, 6783–6796, 2013.

Chow, J. C., Watson, J. G., Crow, D., Lowenthal, D. H., and Merrifield, T.: Comparison of IMPROVE and NIOSH carbon measurements, Aerosol Sci. Tech., 34, 23–34, 2001.

Chung, S. H. and Seinfeld, J. H.: Global distribution and climate forcing of carbonaceous aerosols, J. Geophys. Res.-Atmos., 107, AAC 14-1–AAC 14-33, doi:10.1029/2001jd001397, 2002.

Docherty, K. S., Stone, E. A., Ulbrich, I. M., DeCarlo, P. F., Snyder, D. C., Schauer, J. J., Peltier, R. E., Weber, R. J., Murphy, S. N., Seinfeld, J. H., Grover, B. D., Eatough, D. J., and Jiimenez, J. L.: Apportionment of primary and secondary organic aerosols in southern california during the 2005 study of organic aerosols in riverside (SOAR-1), Environ. Sci. Technol., 42, 7655–7662, doi:10.1021/es8008166, 2008.

Dusanter, S., Vimal, D., Stevens, P. S., Volkamer, R., and Molina, L. T.: Measurements of OH and HO$_2$ concentrations during the MCMA-2006 field campaign – Part 1: Deployment of the Indiana University laser-induced fluorescence instrument, Atmos. Chem. Phys., 9, 1665–1685, doi:10.5194/acp-9-1665-2009, 2009.

Dzepina, K., Volkamer, R. M., Madronich, S., Tulet, P., Ulbrich, I. M., Zhang, Q., Cappa, C. D., Ziemann, P. J., and Jimenez, J. L.: Evaluation of recently-proposed secondary organic aerosol models for a case study in Mexico City, Atmos. Chem. Phys., 9, 5681–5709, doi:10.5194/acp-9-5681-2009, 2009.

Edney, E. O., Kleindienst, T. E., Conver, T. S., McIver, C. D., Corse, E. W., and Weathers, W. S.: Polar organic oxygenates in PM$_{2.5}$ at a southeastern site in the United States, Atmos. Environ., 37, 3947–3965, 2003.

Ensberg, J. J., Hayes, P. L., Jimenez, J. L., Gilman, J. B., Kuster, W. C., de Gouw, J. A., Holloway, J. S., Gordon, T. D., Jathar, S., Robinson, A. L., and Seinfeld, J. H.: Emission factor ratios, SOA mass yields, and the impact of vehicular emissions on SOA formation, Atmos. Chem. Phys., 14, 2383–2397, doi:10.5194/acp-14-2383-2014, 2014.

Ervens, B., Turpin, B. J., and Weber, R. J.: Secondary organic aerosol formation in cloud droplets and aqueous particles (aqSOA): a review of laboratory, field and model studies, Atmos. Chem. Phys., 11, 11069–11102, doi:10.5194/acp-11-11069-2011, 2011.

Fountoukis, C. and Nenes, A.: ISORROPIA II: a computationally efficient thermodynamic equilibrium model for $K^+ - Ca^{2+} - Mg^{2+} - NH_4^+ - Na^+ - SO_4^{2-} - NO_3^- - Cl^- - H_2O$ aerosols, Atmos. Chem. Phys., 7, 4639–4659, doi:10.5194/acp-7-4639-2007, 2007.

Gantt, B., Meskhidze, N., and Carlton, A. G.: The contribution of marine organics to the air quality of the western United States, Atmos. Chem. Phys., 10, 7415–7423, doi:10.5194/acp-10-7415-2010, 2010.

Gaston, C. J., Riedel, T. P., Zhang, Z., Gold, A., Surratt, J. D., and Thornton, J. A.: Reactive Uptake of an Isoprene-derived Epoxydiol to Submicron Aerosol Particles, Environ. Sci. Technol., 48, 11178–11186, 2014.

Gentner, D. R., Isaacman, G., Worton, D. R., Chan, A. W. H., Dallmann, T. R., Davis, L., Liu, S., Day, D. A., Russell, L. M., Wilson, K. R., Weber, R., Guha, A., Harley, R. A., and Goldstein, A. H.: Elucidating secondary organic aerosol from diesel and gasoline vehicles through detailed characterization of organic carbon emissions, P. Natl. Acad. Sci. USA, 109, 18318–18323, doi:10.1073/pnas.1212272109, 2012.

Gentner, D. R., Ford, T. B., Guha, A., Boulanger, K., Brioude, J., Angevine, W. M., de Gouw, J. A., Warneke, C., Gilman, J. B., Ryerson, T. B., Peischl, J., Meinardi, S., Blake, D. R., Atlas, E., Lonneman, W. A., Kleindienst, T. E., Beaver, M. R., Clair, J. M. St., Wennberg, P. O., VandenBoer, T. C., Markovic, M. Z., Murphy, J. G., Harley, R. A., and Goldstein, A. H.: Emissions of organic carbon and methane from petroleum and dairy operations in California's San Joaquin Valley, Atmos. Chem. Phys., 14, 4955–4978, doi:10.5194/acp-14-4955-2014, 2014a.

Gentner, D. R., Ormeño, E., Fares, S., Ford, T. B., Weber, R., Park, J.-H., Brioude, J., Angevine, W. M., Karlik, J. F., and Goldstein, A. H.: Emissions of terpenoids, benzenoids, and other biogenic gas-phase organic compounds from agricultural crops and their potential implications for air quality, Atmos. Chem. Phys., 14, 5393–5413, doi:10.5194/acp-14-5393-2014, 2014b.

Title Page

Abstract | Introduction

Conclusions | References

Tables | Figures

|◄ | ►|

◄ | ►

Back | Close

Full Screen / Esc

Printer-friendly Version

Interactive Discussion

Gerbig, C., Schmitgen, S., Kley, D., Volz-Thomas, A., Dewey, K., and Haaks, D.: An improved fast-response vacuum-UV resonance fluorescence CO instrument, J. Geophys. Res.-Atmos., 104, 1699–1704, 1999.

Geron, C.: Carbonaceous aerosol over a *Pinus taeda* forest in central North Carolina, USA, Atmos. Environ., 43, 959–969, 2009.

Gilman, J. B., Burkhart, J. F., Lerner, B. M., Williams, E. J., Kuster, W. C., Goldan, P. D., Murphy, P. C., Warneke, C., Fowler, C., Montzka, S. A., Miller, B. R., Miller, L., Oltmans, S. J., Ryerson, T. B., Cooper, O. R., Stohl, A., and de Gouw, J. A.: Ozone variability and halogen oxidation within the Arctic and sub-Arctic springtime boundary layer, Atmos. Chem. Phys., 10, 10223–10236, doi:10.5194/acp-10-10223-2010, 2010.

Grell, G. A., Peckham, S. E., Schmitz, R., McKeen, S. A., Frost, G., Skamarock, W. C., and Eder, B.: Fully coupled "online" chemistry within the WRF model, Atmos. Environ., 39, 6957–6975, doi:10.1016/j.atmosenv.2005.04.027, 2005.

Griffith, S. M., Hansen, R. F., Dusanter, S., Stevens, P. S., Alaghmand, M., Bertman, S. B., Carroll, M. A., Erickson, M., Galloway, M., Grossberg, N., Hottle, J., Hou, J., Jobson, B. T., Kammrath, A., Keutsch, F. N., Lefer, B. L., Mielke, L. H., O'Brien, A., Shepson, P. B., Thurlow, M., Wallace, W., Zhang, N., and Zhou, X. L.: OH and HO$_2$ radical chemistry during PROPHET 2008 and CABINEX 2009 – Part 1: Measurements and model comparison, Atmos. Chem. Phys., 13, 5403–5423, doi:10.5194/acp-13-5403-2013, 2013.

Hallquist, M., Wenger, J. C., Baltensperger, U., Rudich, Y., Simpson, D., Claeys, M., Dommen, J., Donahue, N. M., George, C., Goldstein, A. H., Hamilton, J. F., Herrmann, H., Hoffmann, T., Iinuma, Y., Jang, M., Jenkin, M. E., Jimenez, J. L., Kiendler-Scharr, A., Maenhaut, W., McFiggans, G., Mentel, Th. F., Monod, A., Prévôt, A. S. H., Seinfeld, J. H., Surratt, J. D., Szmigielski, R., and Wildt, J.: The formation, properties and impact of secondary organic aerosol: current and emerging issues, Atmos. Chem. Phys., 9, 5155–5236, doi:10.5194/acp-9-5155-2009, 2009.

Hayes, P. L., Ortega, A. M., Cubison, M. J., Froyd, K. D., Zhao, Y., Cliff, S. S., Hu, W. W., Toohey, D. W., Flynn, J. H., Lefer, B. L., Grossberg, N., Alvarez, S., Rappenglueck, B., Taylor, J. W., Allan, J. D., Holloway, J. S., Gilman, J. B., Kuster, W. C., De Gouw, J. A., Massoli, P., Zhang, X., Liu, J., Weber, R. J., Corrigan, A. L., Russell, L. M., Isaacman, G., Worton, D. R., Kreisberg, N. M., Goldstein, A. H., Thalman, R., Waxman, E. M., Volkamer, R., Lin, Y. H., Surratt, J. D., Kleindienst, T. E., Offenberg, J. H., Dusanter, S., Griffith, S., Stevens, P. S., Brioude, J., Angevine, W. M., and Jimenez, J. L.: Organic aerosol composition and sources

Title Page

Abstract | Introduction

Conclusions | References

Tables | Figures

◀ | ▶

◀ | ▶

Back | Close

Full Screen / Esc

Printer-friendly Version

Interactive Discussion

in Pasadena, California, during the 2010 CalNex campaign, J. Geophys. Res.-Atmos., 118, 9233–9257, doi:10.1002/jgrd.50530, 2013.

Hayes, P. L., Carlton, A. G., Baker, K. R., Ahmadov, R., Washenfelder, R. A., Alvarez, S., Rappenglück, B., Gilman, J. B., Kuster, W. C., de Gouw, J. A., Zotter, P., Prévôt, A. S. H., Szidat, S., Kleindienst, T. E., Offenberg, J. H., and Jimenez, J. L.: Modeling the formation and aging of secondary organic aerosols in Los Angeles during CalNex 2010, Atmos. Chem. Phys. Discuss., 14, 32325–32391, doi:10.5194/acpd-14-32325-2014, 2014.

Henderson, B. H., Akhtar, F., Pye, H. O. T., Napelenok, S. L., and Hutzell, W. T.: A database and tool for boundary conditions for regional air quality modeling: description and evaluation, Geosci. Model Dev., 7, 339–360, doi:10.5194/gmd-7-339-2014, 2014.

Henze, D. K. and Seinfeld, J. H.: Global secondary organic aerosol from isoprene oxidation, Geophys. Res. Lett., 33, L09812, doi:10.1029/2006gl025976, 2006.

Hersey, S. P., Craven, J. S., Schilling, K. A., Metcalf, A. R., Sorooshian, A., Chan, M. N., Flagan, R. C., and Seinfeld, J. H.: The Pasadena Aerosol Characterization Observatory (PACO): chemical and physical analysis of the Western Los Angeles basin aerosol, Atmos. Chem. Phys., 11, 7417–7443, doi:10.5194/acp-11-7417-2011, 2011.

Hutzell, W. T., Luecken, D. J., Appel, K. W., and Carter, W. P. L.: Interpreting predictions from the SAPRC07 mechanism based on regional and continental simulations, Atmos. Environ., 46, 417–429, doi:10.1016/j.atmosenv.2011.09.030, 2012.

Jathar, S. H., Gordon, T. D., Hennigan, C. J., Pye, H. O. T., Pouliot, G., Adams, P. J., Donahue, N. M., and Robinson, A. L.: Unspeciated organic emissions from combustion sources and their influence on the secondary organic aerosol budget in the United States, P. Natl. Acad. Sci. USA, 111, 10473–10478, doi:10.1073/pnas.1323740111, 2014.

Jimenez, J. L., Canagaratna, M. R., Donahue, N. M., Prevot, A. S. H., Zhang, Q., Kroll, J. H., DeCarlo, P. F., Allan, J. D., Coe, H., Ng, N. L., Aiken, A. C., Docherty, K. S., Ulbrich, I. M., Grieshop, A. P., Robinson, A. L., Duplissy, J., Smith, J. D., Wilson, K. R., Lanz, V. A., Hueglin, C., Sun, Y. L., Tian, J., Laaksonen, A., Raatikainen, T., Rautiainen, J., Vaattovaara, P., Ehn, M., Kulmala, M., Tomlinson, J. M., Collins, D. R., Cubison, M. J., Dunlea, E. J., Huffman, J. A., Onasch, T. B., Alfarra, M. R., Williams, P. I., Bower, K., Kondo, Y., Schneider, J., Drewnick, F., Borrmann, S., Weimer, S., Demerjian, K., Salcedo, D., Cottrell, L., Griffin, R., Takami, A., Miyoshi, T., Hatakeyama, S., Shimono, A., Sun, J. Y., Zhang, Y. M., Dzepina, K., Kimmel, J. R., Sueper, D., Jayne, J. T., Herndon, S. C., Trimborn, A. M., Williams, L. R., Wood, E. C., Middlebrook, A. M., Kolb, C. E., Baltensperger, U., and

Worsnop, D. R.: Evolution of organic aerosols in the atmosphere, Science, 326, 1525–1529, doi:10.1126/science.1180353, 2009.

Karambelas, A., Pye, H. O. T., Budisulistiorini, S. H., Surratt, J. D., and Pinder, R. W.: Isoprene epoxydiol contribution to urban organic aerosol: evidence from modeling and measurements, Environ. Sci. Technol. Lett., 1, 278–283, 2013.

Kelly, J. T., Baker, K. R., Nowak, J. B., Murphy, J. G., Markovic, M. Z., VandenBoer, T. C., Ellis, R. A., Neuman, J. A., Weber, R. J., and Roberts, J. M.: Fine-scale simulation of ammonium and nitrate over the South Coast Air Basin and San Joaquin Valley of California during CalNex-2010, J. Geophys. Res.-Atmos., 119, 3600–3614, 2014.

Kleindienst, T. E., Conver, T. S., McIver, C. D., and Edney, E. O.: Determination of secondary organic aerosol products from the photooxidation of toluene and their implications in ambient PM$_{2.5}$, J. Atmos. Chem., 47, 79–100, 2004.

Kleindienst, T. E., Jaoui, M., Lewandowski, M., Offenberg, J. H., Lewis, C. W., Bhave, P. V., and Edney, E. O.: Estimates of the contributions of biogenic and anthropogenic hydrocarbons to secondary organic aerosol at a southeastern US location, Atmos. Environ., 41, 8288–8300, doi:10.1016/j.atmosenv.2007.06.045, 2007.

Kleindienst, T. E., Lewandowski, M., Offenberg, J. H., Edney, E. O., Jaoui, M., Zheng, M., Ding, X. A., and Edgerton, E. S.: Contribution of primary and secondary sources to organic aerosol and PM$_{2.5}$ at SEARCH network sites, J. Air Waste Manage., 60, 1388–1399, doi:10.3155/1047-3289.60.11.1388, 2010.

Lewandowski, M., Piletic, I. R., Kleindienst, T. E., Offenberg, J. H., Beaver, M. R., Jaoui, M., Docherty, K. S., and Edney, E. O.: Secondary organic aerosol characterisation at field sites across the United States during the spring–summer period, Int. J. Environ. An. Ch., 93, 1084–1103, 2013.

Lewis, C. W., Klouda, G. A., and Ellenson, W. D.: Radiocarbon measurement of the biogenic contribution to summertime PM-2.5 ambient aerosol in Nashville, TN, Atmos. Environ., 38, 6053–6061, doi:10.1016/j.atmosenv.2004.06.011, 2004.

Liu, S., Ahlm, L., Day, D. A., Russell, L. M., Zhao, Y., Gentner, D. R., Weber, R. J., Goldstein, A. H., Jaoui, M., Offenberg, J. H., Kleindienst, T. E., Rubitschun, C., Surratt, J. D., Sheesley, R. J., and Scheller, S.: Secondary organic aerosol formation from fossil fuel sources contribute majority of summertime organic mass at Bakersfield, J. Geophys. Res.-Atmos., 117, D00V26, doi:10.1029/2012JD018170, 2012.

Mao, J., Ren, X., Zhang, L., Van Duin, D. M., Cohen, R. C., Park, J.-H., Goldstein, A. H., Paulot, F., Beaver, M. R., Crounse, J. D., Wennberg, P. O., DiGangi, J. P., Henry, S. B., Keutsch, F. N., Park, C., Schade, G. W., Wolfe, G. M., Thornton, J. A., and Brune, W. H.: Insights into hydroxyl measurements and atmospheric oxidation in a California forest, Atmos. Chem. Phys., 12, 8009–8020, doi:10.5194/acp-12-8009-2012, 2012.

Markovic, M., VandenBoer, T., Baker, K., Kelly, J., and Murphy, J.: Measurements and modeling of the inorganic chemical composition of fine particulate matter and associated precursor gases in California's San Joaquin Valley during CalNex 2010, J. Geophys. Res.-Atmos., 119, 6853–6866, 2014.

Offenberg, J. H., Lewandowski, M., Edney, E. O., Kleindienst, T. E., and Jaoui, M.: Influence of aerosol acidity on the formation of secondary organic aerosol from biogenic precursor hydrocarbons, Environ. Sci. Technol., 43, 7742–7747, doi:10.1021/es901538e, 2009.

Ormeño, E., Gentner, D. R., Fares, S., Karlik, J., Park, J. H., and Goldstein, A. H.: Sesquiter-penoid emissions from agricultural crops: correlations to monoterpenoid emissions and leaf terpene content, Environ. Sci. Technol., 44, 3758–3764, 2010.

Pye, H. O. T. and Pouliot, G. A.: Modeling the role of alkanes, polycyclic aromatic hydrocarbons, and their oligomers in secondary organic aerosol formation, Environ. Sci. Technol., 46, 6041–6047, doi:10.1021/es300409w, 2012.

Pye, H. O., Pinder, R. W., Piletic, I. R., Xie, Y., Capps, S. L., Lin, Y.-H., Surratt, J. D., Zhang, Z., Gold, A., and Luecken, D. J.: Epoxide pathways improve model predictions of isoprene markers and reveal key role of acidity in aerosol formation, Environ. Sci. Technol., 47, 11056–11064, 2013.

Robinson, A. L., Donahue, N. M., Shrivastava, M. K., Weitkamp, E. A., Sage, A. M., Grieshop, A. P., Lane, T. E., Pierce, J. R., and Pandis, S. N.: Rethinking organic aerosols: semivolatile emissions and photochemical aging, Science, 315, 1259–1262, 2007.

Rollins, A., Browne, E., Min, K.-E., Pusede, S., Wooldridge, P., Gentner, D., Goldstein, A., Liu, S., Day, D., and Russell, L.: Evidence for NO_x control over nighttime SOA formation, Science, 337, 1210–1212, 2012.

Ryerson, T. B., Andrews, A. E., Angevine, W. M., Bates, T. S., Brock, C. A., Cairns, B., Cohen, R. C., Cooper, O. R., de Gouw, J. A., Fehsenfeld, F. C., Ferrare, R. A., Fischer, M. L., Flagan, R. C., Goldstein, A. H., Hair, J. W., Hardesty, R. M., Hostetler, C. A., Jimenez, J. L., Langford, A. O., McCauley, E., McKeen, S. A., Molina, L. T., Nenes, A., Oltmans, S. J., Parrish, D. D., Pederson, J. R., Pierce, R. B., Prather, K., Quinn, P. K., Seinfeld, J. H.,

Title Page

Abstract	Introduction
Conclusions	References
Tables	Figures

|◄ | ►|

◄ | ►

Back | Close

Full Screen / Esc

Printer-friendly Version

Interactive Discussion

Senff, C. J., Sorooshian, A., Stutz, J., Surratt, J. D., Trainer, M., Volkamer, R., Williams, E. J., and Wofsy, S. C.: The 2010 California research at the nexus of air quality and climate change (CalNex) field study, J. Geophys. Res.-Atmos., 118, 5830–5866, doi:10.1002/jgrd.50331, 2013.

5 Sarwar, G., Fahey, K., Kwok, R., Gilliam, R. C., Roselle, S. J., Mathur, R., Xue, J., Yu, J., and Carter, W. P. L.: Potential impacts of two SO_2 oxidation pathways on regional sulfate concentrations: aqueous-phase oxidation by NO_2 and gas-phase oxidation by stabilized criegee intermediates, Atmos. Environ., 68, 186–197, doi:10.1016/j.atmosenv.2012.11.036, 2013.

Shilling, J. E., Zaveri, R. A., Fast, J. D., Kleinman, L., Alexander, M. L., Canagaratna, M. R., Fort-
10 ner, E., Hubbe, J. M., Jayne, J. T., Sedlacek, A., Setyan, A., Springston, S., Worsnop, D. R., and Zhang, Q.: Enhanced SOA formation from mixed anthropogenic and biogenic emissions during the CARES campaign, Atmos. Chem. Phys., 13, 2091–2113, doi:10.5194/acp-13-2091-2013, 2013.

Simon, H. and Bhave, P. V.: Simulating the degree of oxidation in atmospheric organic particles,
15 Environ. Sci. Technol., 46, 331–339, doi:10.1021/es202361w, 2012.

Steiner, A. L., Cohen, R. C., Harley, R. A., Tonse, S., Millet, D. B., Schade, G. W., and Goldstein, A. H.: VOC reactivity in central California: comparing an air quality model to ground-based measurements, Atmos. Chem. Phys., 8, 351–368, doi:10.5194/acp-8-351-2008, 2008.

20 Stuiver, M.: International agreements and the use of the new oxalic acid standard, Radiocarbon, 25, 793–795, 1983.

Tan, Y., Carlton, A. G., Seitzinger, S. P., and Turpin, B. J.: SOA from methylglyoxal in clouds and wet aerosols: measurement and prediction of key products, Atmos. Environ., 44, 5218–5226, doi:10.1016/j.atmosenv.2010.08.045, 2010.

25 United States Environmental Protection Agency, The 2011 National Emissions Inventory, http://www.epa.gov/ttnchie1/net/2011inventory.html, last access: 1 October 2014.

Washenfelder, R. A., Young, C. J., Brown, S. S., Angevine, W. M., Atlas, E. L., Blake, D. R., Bon, D. M., Cubison, M. J., de Gouw, J. A., Dusanter, S., Flynn, J., Gilman, J. B., Graus, M., Griffith, S., Grossberg, N., Hayes, P. L., Jimenez, J. L., Kuster, W. C., Lefer, B. L., Pollack, I. B.,
30 Ryerson, T. B., Stark, H., Stevens, P. S., and Trainer, M. K.: The glyoxal budget and its contribution to organic aerosol for Los Angeles, California, during CalNex 2010, J. Geophys. Res.-Atmos., 116, D00V02, doi:10.1029/2011jd016314, 2011.

Yarwood, G., Rao, S., Yocke, M., and Whitten, G. Z.: Updates to the Carbon Bond Chemical Mechanism: CB05, ENVIRON International Corporation, Novato, CA, 2005.

Zhang, H., Chen, G., Hu, J., Chen, S.-H., Wiedinmyer, C., Kleeman, M., and Ying, Q.: Evaluation of a seven-year air quality simulation using the weather research and forecasting (WRF)/community multiscale air quality (CMAQ) models in the eastern United States, Sci. Total Environ., 473, 275–285, 2014a.

Zhang, X., Cappa, C. D., Jathar, S. H., McVay, R. C., Ensberg, J. J., Kleeman, M. J., and Seinfeld, J. H.: Influence of vapor wall loss in laboratory chambers on yields of secondary organic aerosol, P. Natl. Acad. Sci. USA, 111, 5802–5807, 2014b.

Zhao, Y., Kreisberg, N. M., Worton, D. R., Isaacman, G., Gentner, D. R., Chan, A. W., Weber, R. J., Liu, S., Day, D. A., and Russell, L. M.: Sources of organic aerosol investigated using organic compounds as tracers measured during CalNex in Bakersfield, J. Geophys. Res.-Atmos., 118, 11388–11398, 2013.

Zotter, P., El-Haddad, I., Zhang, Y., Hayes, P. L., Zhang, X., Lin, Y. H., Wacker, L., Schnelle-Kreis, J., Abbaszade, G., and Zimmermann, R.: Diurnal cycle of fossil and nonfossil carbon using radiocarbon analyses during CalNex, J. Geophys. Res.-Atmos., 119, 6818–6835, 2014.

Table 1. Episode total anthropogenic emissions of primarily emitted $PM_{2.5}$ organic carbon and the sum of benzene, toluene, and xylenes by emissions sector group. The Los Angeles (LA) total includes Los Angeles and Orange counties. The southern San Joaquin Valley (SSJV) total includes Kern, Fresno, Kings, and Tulare counties. Green shading indicates the sector group for that location is mostly contemporary in origin.

Sector	Primarily emitted $PM_{2.5}$ organic carbon				Benzene + Toluene + Xylenes			
	SSJV (tons)	SSJV (%)	LA (tons)	LA (%)	SSJV (tons)	SSJV (%)	LA (tons)	LA (%)
Non-point area	139.9	33.8	410.1	40.8	326.7	37.2	1229.3	35.8
Onroad mobile	73.3	17.7	263.6	26.2	273.5	31.2	1190.9	34.6
Nonroad mobile	23.9	5.8	161.4	16.1	170.1	19.4	822.3	23.9
Point: non-electrical generating	61.3	14.8	56.3	5.6	68.3	7.8	177.7	5.2
Residential wood combustion	54.1	13.1	82.7	8.2	2.0	0.2	3.2	0.1
Oil & gas exploration and related	28.5	6.9	0.0	0.0	34.2	3.9	1.1	0.0
Fugitive dust	24.9	6.0	18.1	1.8	0.0	0.0	0.0	0.0
Commercial marine & rail	3.8	0.9	11.4	1.1	2.6	0.3	12.8	0.4
Point: electrical generating	4.3	1.0	1.7	0.2	0.1	0.0	1.0	0.0
Total Contemporary Carbon	218.9	52.9	510.9	50.8	2.0	0.2	3.2	0.1
Total Fossil Carbon	195.2	47.1	494.5	49.2	875.3	99.8	3435.1	99.9

Table 2. Episode average measured and modeled $PM_{2.5}$ carbon, $PM_{2.5}$ SOC groups, and VOC at the Pasadena and Bakersfield sites.

Specie	Model Run	Location	N	Observed ($\mu g\,C\,m^{-3}$)	Predicted ($\mu g\,C\,m^{-3}$)	Bias ($\mu g\,C\,m^{-3}$)	Error ($\mu g\,C\,m^{-3}$)	Fractional Bias (%)	Fractional Error (%)
Elemental Carbon	Baseline	Bakersfield	35	0.5	0.4	−0.1	0.1	−13	35
	Baseline	Pasadena	31	0.2	1	0.8	0.8	125	125
	Baseline	33 CSN/IMPROVE sites	531	0.2	0.3	0.2	0.2	27	70
Organic Carbon	Baseline	Bakersfield	35	5.4	0.8	−4.6	4.6	−144	144
	Baseline	Pasadena	31	3.6	2	−1.6	1.6	−53	53
	Baseline	33 CSN/IMPROVE sites	531	1.2	0.7	−0.5	0.6	−63	75
	Sensitivity	33 CSN/IMPROVE sites	531	1.2	1.0	−0.1	0.5	−25	51

Specie	Model Run	Location	N	Observed ($ng\,C\,m^{-3}$)	Predicted ($ng\,C\,m^{-3}$)	Bias ($ng\,C\,m^{-3}$)	Error ($ng\,C\,m^{-3}$)	Fractional Bias (%)	Fractional Error (%)
Isoprene SOC	Baseline	Bakersfield	36	96	21	−75	75	−126	128
		Pasadena	32	42	27	−15	25	−60	83
Monoterpene SOC	Baseline	Bakersfield	35	55	21	−35	37	−75	89
		Pasadena	32	82	21	−60	61	−89	93
Toluene + Xylene SOC	Baseline	Bakersfield	35	57	15	−44	44	−114	114
		Pasadena	32	125	36	−89	89	−100	100
Sesquiterpene SOC	Baseline	Bakersfield	43		17				
		Pasadena	43		7				
Benzene SOC	Baseline	Bakersfield	43		2				
		Pasadena	43		2				
Alkane SOC	Baseline	Bakersfield	43		12				
		Pasadena	43		22				
Cloud SOC	Baseline	Bakersfield	43		1				
		Pasadena	43		5				
Naphthalene SOC	Baseline	Bakersfield	36	43					
		Pasadena	30	114					

Title Page

Abstract | Introduction

Conclusions | References

Tables | Figures

◄ | ►►

◄ | ►

Back | Close

Full Screen / Esc

Printer-friendly Version

Interactive Discussion

Table 2. Continued.

| Specie	Model Run	Location	N	Observed (ppb C)	Predicted (ppb C)	Bias (ppb C)	Error (ppb C)	Fractional Bias (%)	Fractional Error (%)
Isoprene VOC 3 h	Baseline	Bakersfield	5	0.1	0.3	0.2	0.2	82	82
		Pasadena	8	0.6	0.5	−0.1	0.5	2	84
Monoterpene VOC 3 h	Baseline	Bakersfield	37	1.4	0.5	−0.9	1	−70	87
		Pasadena	28	1.8	0.3	−1.5	1.5	−125	133
Toluene VOC 3 h	Baseline	Bakersfield	41	4.3	2.7	−1.6	1.9	−47	54
		Pasadena	29	7.3	7.8	0.5	3.5	18	44
Xylene VOC 3 h	Baseline	Bakersfield	41	4.3	1.9	−2.5	2.5	−81	82
		Pasadena	29	6.7	4.6	−2.1	2.6	−32	40
Benzene VOC 3 h	Baseline	Bakersfield	41	1.2	1.3	0.2	0.5	7	37
		Pasadena	29	1.5	1.6	0.1	0.5	2	30
Total VOC 3 h	Baseline	Bakersfield	41	186.9	63.8	−123.1	124.1	−95	97
		Pasadena	29	188.9	89.5	−99.4	99.5	−65	65
Isoprene VOC 1 h	Baseline	Bakersfield	712	0.4	0.4	0	0.4	−15	82
		Pasadena	718	1.6	0.8	−0.8	1.8	−30	139
Monoterpene VOC 1 h	Baseline	Bakersfield	605	0.8	0.3	−0.5	0.7	−60	99
		Pasadena	707	0.7	0.2	−0.5	0.5	−98	106
Toluene VOC 1 h	Baseline	Bakersfield	737	2.5	1.7	−0.8	1.5	−23	56
		Pasadena	717	4	6.2	2.1	2.8	38	54
Xylene VOC 1 h	Baseline	Bakersfield	737	1.9	1.2	−0.7	1.2	−34	63
		Pasadena	718	3.2	3.5	0.3	1.7	6	50

Title Page

Abstract | Introduction

Conclusions | References

Tables | Figures

◄◄ | ►►

◄ | ►

Back | Close

Full Screen / Esc
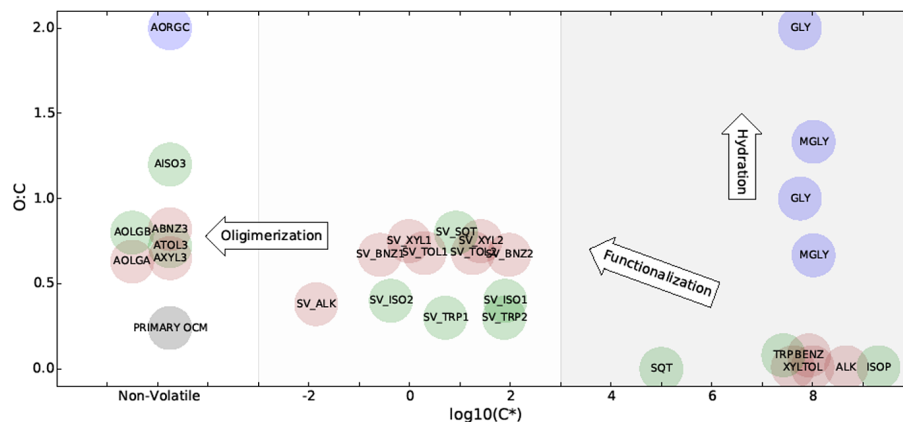
Figure 1. Gas (right panel), semi-volatile (middle panel), and particle phase (left panel) CMAQ organic carbon shown by saturation vapor pressure and O : C ratio. Compounds shown in blue exist in the aqueous phase, brown suggest generally fossil in origin, green generally contemporary in origin, and gray both contemporary and fossil in origin. Other known processes such as fragmentation are not shown as they are not currently represented in the modeling system.
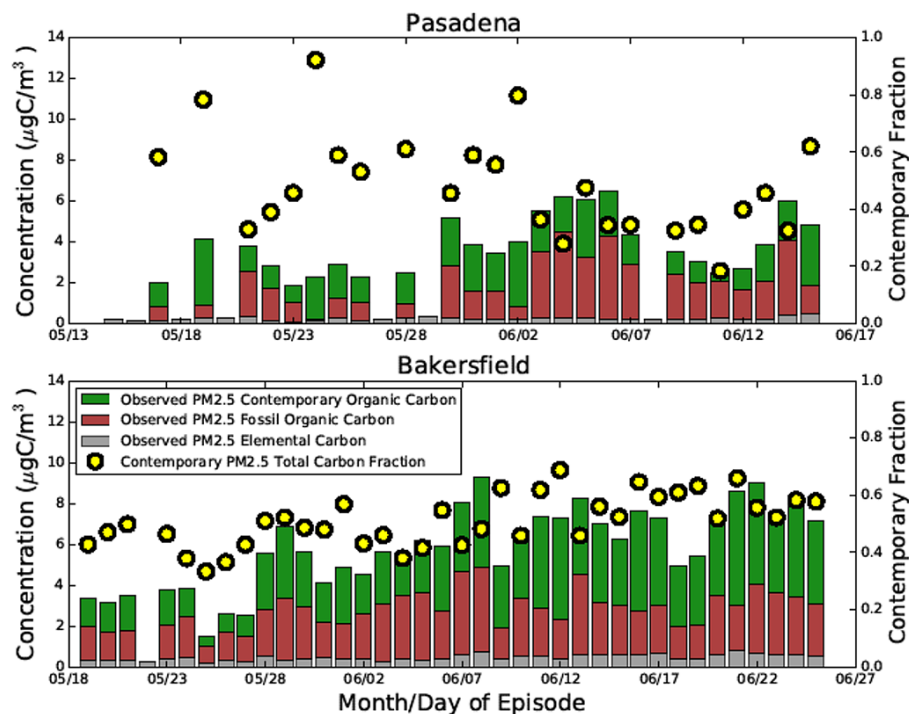
Figure 2. Observed daily 23 h average total carbon and contemporary total carbon fraction at Pasadena and Bakersfield.
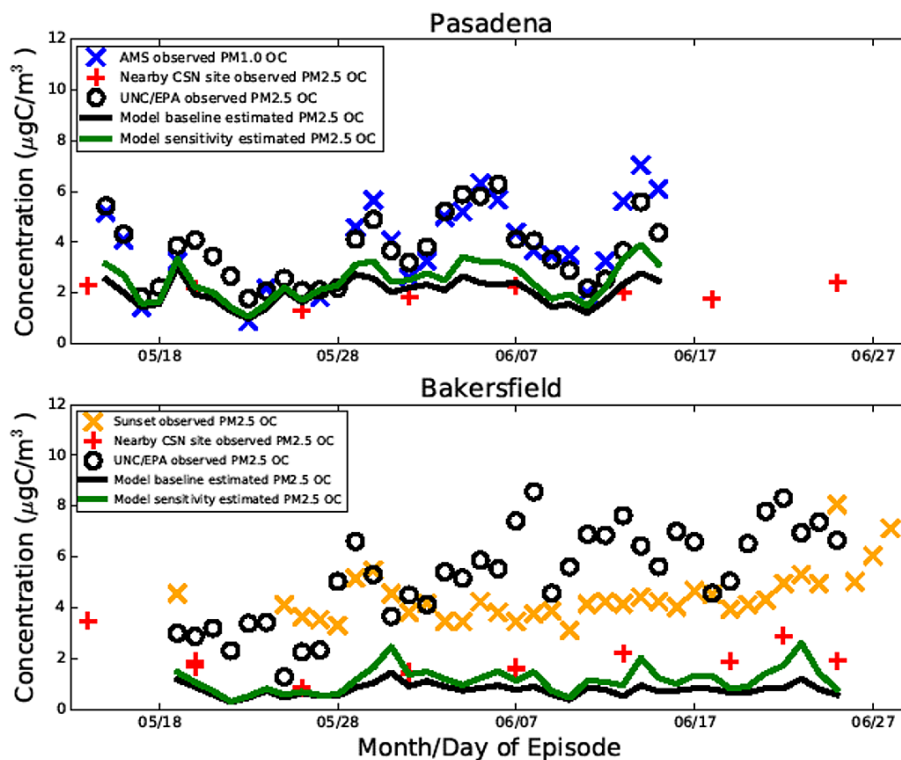
Figure 3. Model predicted and measured PM organic carbon at Pasadena and Bakersfield. The nearby CSN measurements are intended to provide additional context and are not co-located with CalNex measurements or model estimates.
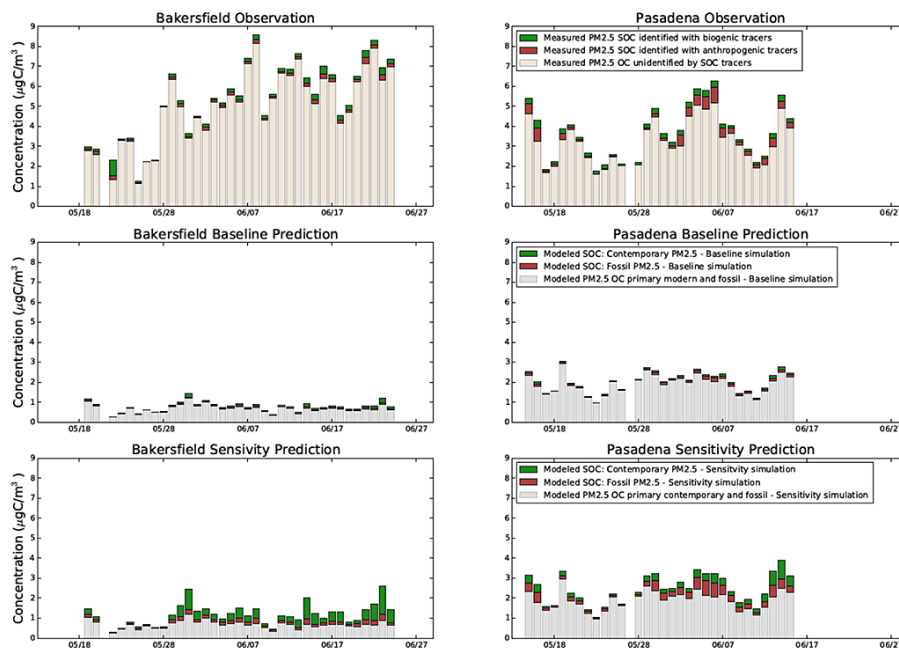
Figure 4. Observed (top row) and modeled (middle and bottom row) PM$_{2.5}$ organic carbon at Pasadena and Bakersfield. Mass explained by SOA tracers shown in green (contemporary origin tracers) and brown (fossil origin tracers). Gray shading indicates mass not explained by known SOC tracers for observations and primarily emitted PM$_{2.5}$ (both contemporary and fossil) for modeled estimates. Middle row shows baseline model estimates and bottom row model sensitivity results with increased SOA yields.
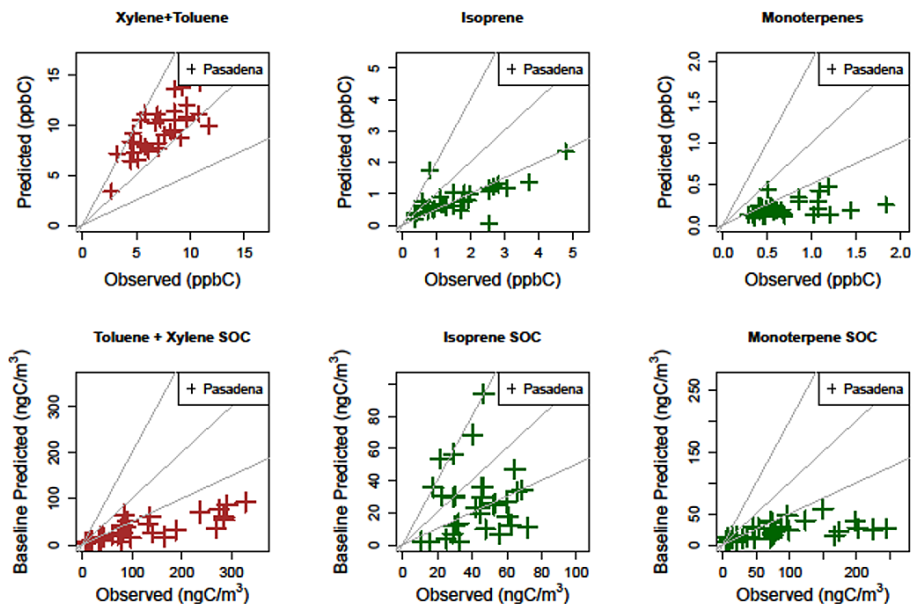
Figure 5. Comparison of CMAQ-predicted and measured VOC (daily average of hourly samples) and corresponding SOC species (daily 23 h average samples) for Pasadena. Comparison points outside the gray lines indicate model predictions are greater than a factor of 2 different from the measurements.
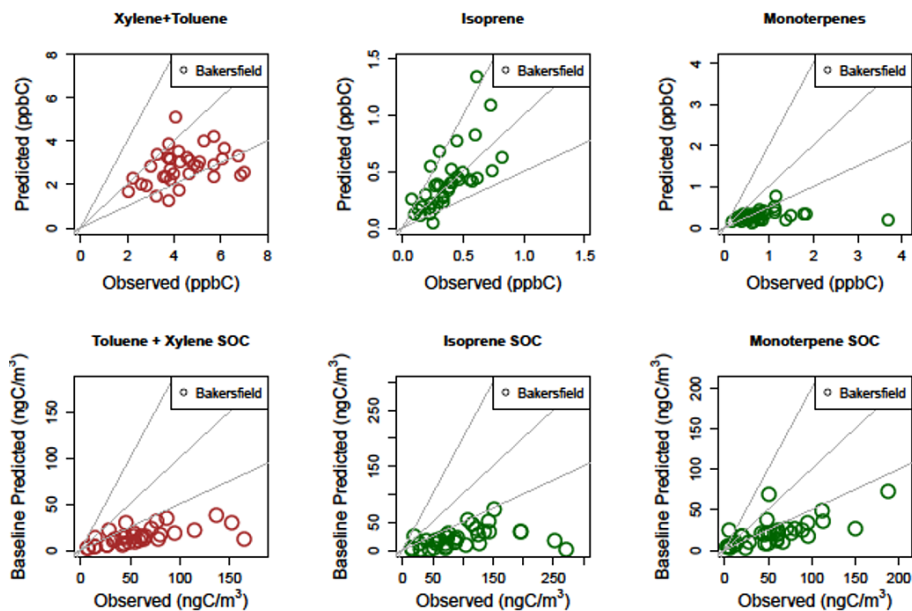
Figure 6. Comparison of CMAQ-predicted and measured VOC (daily average of hourly samples) and corresponding SOC species (daily 23 h average samples) for Bakersfield. Comparison points outside the gray lines indicate model predictions are greater than a factor of 2 different from the measurements.
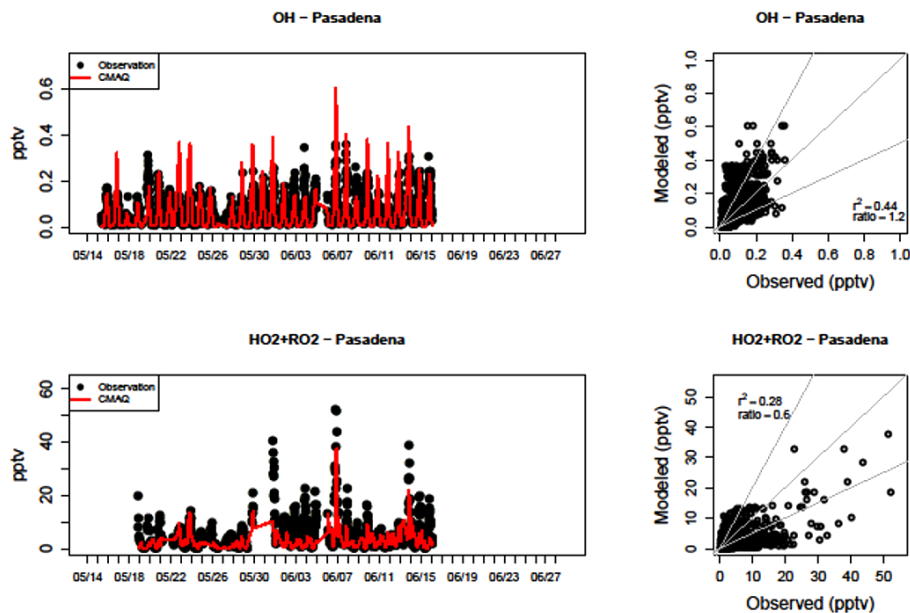
Figure 7. Measured and model estimated OH radical (top) and $HO_2 + RO_2$ (bottom) at Pasadena. The ratio shown on the scatterplots is the episode average model estimates divided by the episode average measured values.
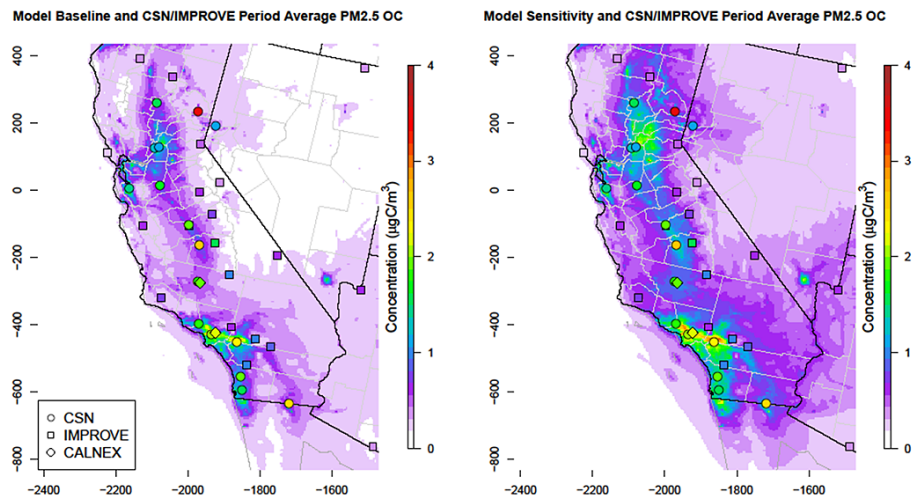
Figure 8. May–June 2010 average observed and modeled PM$_{2.5}$ organic carbon. Measurements from both CalNex locations and routine networks including CSN (circles) and IMPROVE (squares). Left panel shows baseline model predictions and right panel shows model estimates with increased SOA yields.